Geophysical Research Letters

Key Points:
- Injecting in autumn results in more precipitation over India than annually constant injection and increases Arctic September sea ice
- Injecting in spring results in less precipitation changes over the Amazon Basin and requires much less SO_2 to cool the surface
- Underlying trade-offs exist between strategies that meet different regional objectives: this has implications for any governance effort

Supporting Information:
- Supporting Information S1

Correspondence to:
D. Visioni,
daniele.visioni@cornell.edu

Seasonally Modulated Stratospheric Aerosol Geoengineering Alters the Climate Outcomes

Daniele Visioni[1] , Douglas G. MacMartin[1] , Ben Kravitz[2,3] , Jadwiga H. Richter[4] , Simone Tilmes[5] , and Michael J. Mills[5]

[1]Sibley School for Mechanical and Aerospace Engineering, Cornell University, Ithaca, NY, USA, [2]Department of Earth and Atmospheric Science, Indiana University, Bloomington, IN, USA, [3]Atmospheric Sciences and Global Change Division, Pacific Northwest National Laboratory, Richland, WA, USA, [4]Climate and Global Dynamics Laboratory, National Center for Atmospheric Research, Boulder, CO, USA, [5]Atmospheric Chemistry, Observations, and Modeling Laboratory, National Center for Atmospheric Research, Boulder, CO, USA

Abstract By reflecting some incoming solar radiation, stratospheric aerosol intervention using SO_2 would reduce global mean temperature. Previous research has shown that multiple injection latitudes can be used to maintain not only global mean temperature, but also interhemispheric and equator-to-pole temperature gradients. However, the regional climate response depends not only on where the SO_2 is injected, but also on when. We show here that even with these same objectives and same choices of latitudes, injecting in only one season instead of continuously throughout the year results in significant differences in regional climate, for instance in the magnitude of precipitation changes over India. The differential outcomes highlight the potential for underlying trade-offs, with different choices regarding deployment leading to a different distribution of benefits or harms. This aspect of climate engineering should be considered in developing governance and emphasizes the need for a deeper understanding of the mechanisms underlying the regional responses.

Plain Language Summary Injecting sulfate in the stratosphere has been suggested as a quick, temporary solution to the warming produced by the increase in greenhouse gases. This method would however come with some drawback that could become important at a regional scale. We show here that some of what are considered drawbacks of sulfate injection interventions (a reduction in precipitation over India or the Amazon Basin, or an imperfect recovery of sea ice at high northern latitudes) are dependent on the strategy used (injecting all year round versus injecting in only one season per each hemisphere). The presence of regional trade-offs between different strategies indicates that this is an important point when considering an eventual global governance of this method.

1. Introduction

Various model simulations have shown that injecting sulfate in the stratosphere (sulfate aerosol geoengineering [SAG]) has the potential to offset some or all of the warming that will be produced by the increase in greenhouse gases (GHGs) in the 21st century and beyond (Lawrence et al., 2018; National Research Council, 2015; Tilmes, Richter, Kravitz, et al., 2018). The idea of using sulfate aerosols to achieve the cooling (Crutzen, 2006) stems from the observation of past explosive volcanic eruptions that were followed by a period of surface cooling due to the optically thick cloud of aerosols generated by the injected SO_2 (Robock, 2000). Global and annual cooling can be achieved through SAG, but because SAG imperfectly compensates radiative forcing from the CO_2, the climate is not restored to a previous state, especially from a hydrological perspective, both in more idealized scenarios (using solar dimming as a proxy, Niemeier et al., 2013; Tilmes et al., 2013) and under a scenario with a more realistic representation of the stratospheric aerosols (Cheng et al., 2019; Simpson et al., 2019).

Furthermore, the presence of the aerosols would also heat the stratosphere due to absorption of solar near-infrared radiation (Labitzke & McCormick, 1992; Pitari et al., 2016), affecting surface climate, with notable winter warming over Eurasia (Fasullo et al., 2018; Jiang et al., 2019; Zambri & Robock, 2016) as well as a potential role in hydrological changes (Simpson et al., 2019). Stratospheric chemistry would also be

affected, in particular ozone and methane (Pitari et al., 2014; Richter et al., 2017; Tilmes, Richter, Mills, et al., 2018; Visioni, Pitari, Aquila, Tilmes, et al., 2017).

Undesired climate impacts are therefore impossible to avoid completely under an SAG scenario. The question that remains open is the possibility to design SAG strategies that minimize detrimental climate impacts (Kravitz et al., 2016; MacMartin et al., 2013). By combining injections at different latitudes, it is possible in climate simulations to achieve different aerosol optical depth (AOD) patterns and responses in the surface temperature (MacMartin et al., 2017), and thus, more than one climate goal can be achieved, as suggested by Ban-Weiss and Caldeira (2010) and Kravitz et al. (2016) and shown in Kravitz et al. (2017) and Tilmes, Richter, Kravitz, et al. (2018).

Past simulations have applied constant injection rates throughout the year. However, the stratospheric circulation varies seasonally, and the incoming solar radiation varies seasonally, motivating the potential for exploring seasonally dependent injection rates as suggested (but using solar reduction) by MacMartin et al. (2013). Using short-term, single-location injections, Visioni et al. (2019) have shown that limiting the injection of stratospheric sulfate to only one season can improve efficiency (AOD per Tg-SO_2 injected) over annual injections of the same magnitude and motivates the current work by indicating the ability to achieve additional spatiotemporal patterns of solar reduction. For example, injection in Northern Hemisphere autumn (September, October, and November [SON]) results in higher AOD over the Arctic during the summer melt season than either annually constant injection or spring injection of the same amount, suggesting that autumn injection might better recover Arctic sea ice.

Here we conduct and analyze new simulations to explore the climate response to seasonal injection. Similar to the Geoengineering Large Ensemble (GLENS, Tilmes, Richter, Kravitz, et al., 2018), we simulate stratospheric sulfate injection strategies aimed at meeting three different climate objectives: keeping global mean surface temperatures, equator-to-pole temperature gradient, and interhemispheric temperature gradient all at 2020 levels under an RCP8.5 scenario. However, rather than annually constant injection rates, we consider injections in only one season at a time. Even for injection strategies that achieve broadly similar results at a global scale, there can be significant differences at regional scale that depend on the timing of injection. We focus in particular on Arctic sea ice extent, monsoonal precipitation over India, and dry-season precipitation over the Amazon. There is the potential for different choices to lead to important differences at a regional scale even when the global-scale response is similar, highlighting the need to recognize temporal variations when making broad statements about what SAG might or might not do.

2. Methods

For comparison with the simulations analyzed herein, we use the 21-member simulations from GLENS, performed with the Community Earth System Model (CESM1) with the Whole Atmosphere Community Climate Model (WACCM). The GLENS 21-member ensemble (Tilmes, Richter, Mills, et al., 2018) is here named iANNUAL to signify that the injection rates are constant throughout each year. GLENS simulations use an RCP8.5 background emission scenario and start in 2020 up until 2100, and the feedback algorithm (Kravitz et al., 2017; MacMartin et al., 2017) aims to maintain the first three degrees of freedom of the annual mean and zonal mean surface temperature: T_0, (global surface temperatures), T_1 (equator-to-pole gradient), and T_2 (interhemispheric gradient), defined as

$$T_0 = \frac{1}{A}\int_\psi T(\psi)dA \qquad dA = cos(\psi)d\psi$$

$$T_1 = \frac{1}{A}\int_\psi sin(\psi)T(\psi)dA$$

$$T_2 = \frac{1}{A}\int_\psi \frac{1}{2}(3sin^2(\psi)-1)T(\psi)dA$$

at the same values as the reference (2010–2029) period. The projection of the AOD onto the same three bases is denoted L_0, L_1, and L_2. The feedback algorithm decides every year how much SO_2 to inject at each of four different locations (30°S, 15°S, 15°N, 30°N) 5 km above the average tropopause height to maintain the mentioned climate goals.

Table 1
Summary of Experiments Analyzed in This Paper

Run name	Ensemble size	Season of injection (NH)	Season of injection (SH)
iANNUAL	21	1 January to 31 December	1 January to 31 December
iAUTUMN	3	1 September to 30 November	1 March to 31 May
iSPRING	3	1 March to 31 May	1 September to 30 November

For this work, we run two new ensembles of simulations branching from the first members of the GLENS ensemble in 2060, where, instead of injecting SO_2 annually, we shift the strategy to inject in just one season. For this reason, the ensembles are called iAUTUMN and iSPRING, in relation to the injection happening in the related season in each hemisphere (see Table 1). For all ensembles, we analyze the period 2070–2089, using the years from 2060 to 2069 as spin-up to give time for the algorithm (and the climate) to converge to the new state. These two seasons yield the largest differences relative to annual injection; select results for iWINTER and iSUMMER are shown in the Supporting Information as they are roughly intermediate between the iAUTUMN and iSPRING simulations.

The model used in all simulations has been described and validated for past volcanic eruptions by Mills et al. (2016, 2017), here using CLM4.5 as its land model instead, as in GLENS. The model grid is 0.9° latitude × 1.25° longitude, with 70 vertical layers and a model top at 140 km. Sulfate aerosol microphysics is treated with a modal approach using three modes (Liu et al., 2012).

3. Results

3.1. Differences in Injection

A first observation, as expected from Visioni et al. (2019), is that limiting injection to only one season results in less SO_2 injection needed to achieve a similar global AOD value (Figure 1a), since every year, the injection happens in a location where most aerosols have been already transported away (Figure S1), and therefore, the SO_2 can nucleate into new smaller particles rather than coagulating into preexisting particles. For iSPRING, this results in 23% less SO_2 needed per year compared with iANNUAL, with obvious benefits in reduced sulfate deposition (Visioni et al., 2018).

The feedback algorithm results in similar annual mean values for the global mean temperature, as well as the interhemispheric and equator-to-pole temperature gradients (T_0, T_1, T_2). While the distribution of SO_2 injection rates across the four latitudes differs slightly across the different simulations, the resulting annual mean values for the global mean AOD, the interhemispheric distribution of AOD, and equator-to-pole AOD gradients (L_0, L_1, L_2) are all similar. However, even in the iANNUAL case, the AOD varies seasonally due to the differences in stratospheric circulation (Visioni et al., 2019, see also Figure S1). While limiting injection to just one of the seasons results in similar annual mean values, it leads to significant differences in the seasonal dependence of the AOD. This in turn can influence surface climate, as we will show below. While some differences are present also in the stratospheric distribution of sulfate (Figure S2), their effect on stratospheric temperatures is small (Figure S3) and does not influence the changes of key stratospheric variables (i.e., ozone). In the case of iSPRING, a reduced amount of stratospheric water vapor is advected from the troposphere to the stratosphere due to less warming close to the tropopause (Figure S3, Visioni, Pitari, & Aquila, 2017), resulting in a smaller global value of AOD (Table 2).

3.2. Differences in Surface Climate

The annually averaged surface temperatures demonstrate that all three injection strategies achieve the basic goal of mitigating the warming produced by the increase in CO_2. However, the assessment of the resulting changes in climate must also consider other factors, such as changes in precipitation (Simpson et al., 2019) or in temperatures and sea ice at high latitudes (Jiang et al., 2019).

In our simulations, in many places, the surface climate is not significantly different among the different simulations: for instance, precipitation changes in Africa, Europe, and North America do not seem significantly different between the three injection strategies (Figure S5). There are, however, some areas where differences are notable, on which we'll focus below: Arctic sea ice and precipitation changes in the monsoon
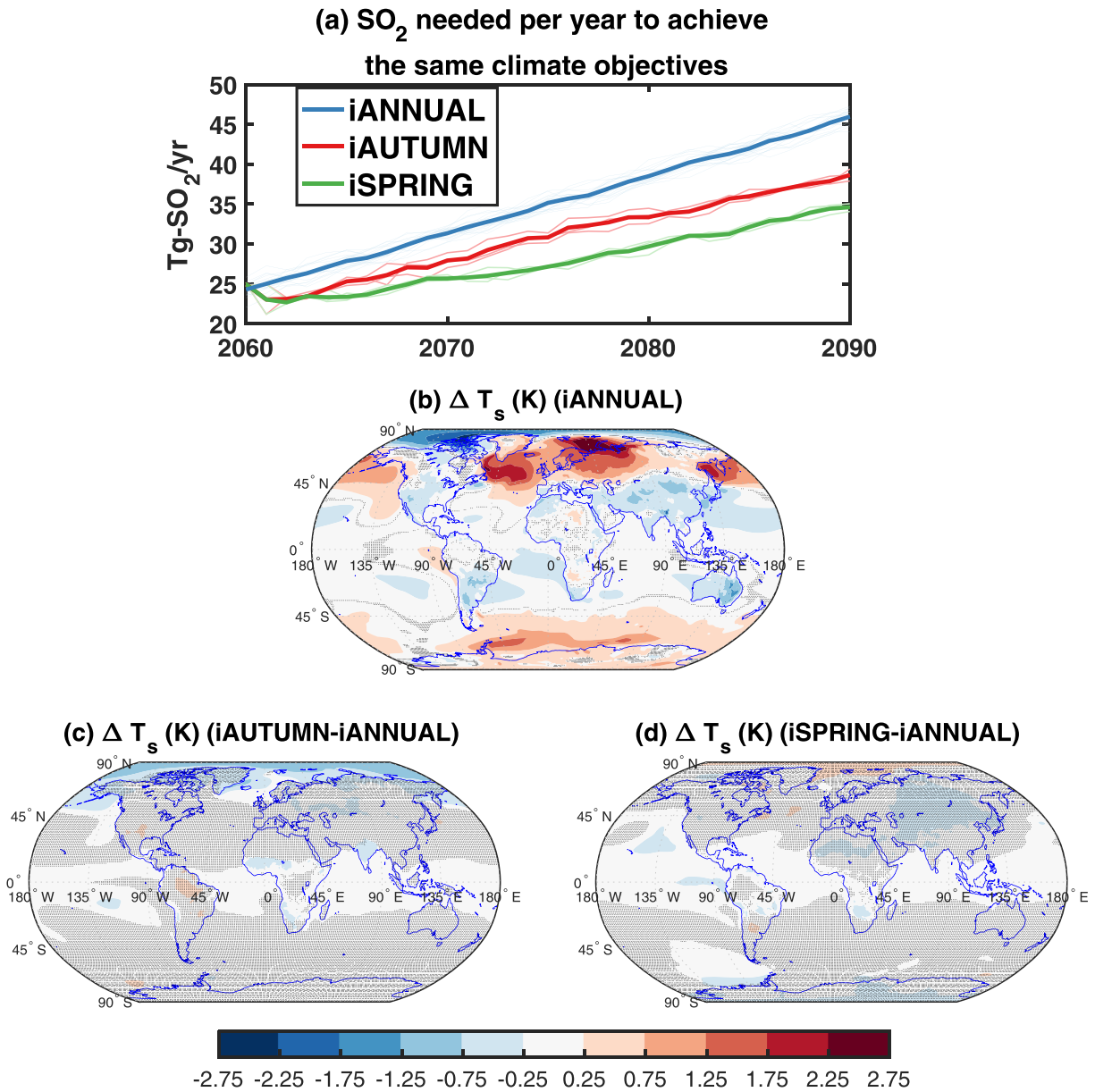
Figure 1. (a) Amount of SO$_2$ injected at all four locations for the three injection strategies. Light lines represent single ensemble members, while thick lines represent the ensemble average. Annually averaged temperatures (K) for the 2070 and 2089 period compared with the control period for iANNUAL (b) and for iAUTUMN-iANNUAL (c) and iSPRING-iANNUAL (d). Gray areas indicate regions where the differences are not significantly different from zero (p value < 0.05) using a two-sided t test.

season over India and in the dry season over the Amazon Basin. This does not exclude the possibility of other differences being present relating to other parameters of the surface climate in other parts of the world and merely hopes to give an example of possible trade-offs in the climate system when analyzing different strategies.

At high latitudes, the month when the peak AOD is reached and the months with highest solar irradiance influence the ability of SAG to recover sea ice extent. For iAUTUMN, the peak AOD at high latitudes occurs during the early melt season (Figure 2) from March through June, while relative to iANNUAL, the iSPRING case results in less AOD during these months and higher AOD from October through January. As a result, iAUTUMN leads to greater recovery in sea ice from July through August, while iSPRING results in the least summer sea ice recovery. The under-recovery of winter sea ice is however present in all simulations, since it is due to the dynamical effect of the stratospheric heating produced by the aerosols, as shown in Jiang

Table 2
Comparison of Various Metrics for Three Injection Strategies

Metric		iANNUAL	iAUTUMN	iSPRING
Average SO_2 injected per year (Tg)		38.9 ± 0.6	33.8 ± 1.5	30.0 ± 1.1
Global AOD (L_0)		0.475 ± 0.001	0.474 ± 0.004	0.467 ± 0.003
Interhemispheric gradient of AOD (L_1)		0.105 ± 0.001	0.096 ± 0.005	0.106 ± 0.005
Euator-to-pole gradient of AOD (L_2)		0.262 ± 0.002	0.243 ± 0.007	0.238 ± 0.009
Surface temperature (K)	T_0 change	0.053 ± 0.001	-0.021 ± 0.003	-0.041 ± 0.003
	T_1 change	0.015 ± 0.001	-0.020 ± 0.002	0.002 ± 0.003
	T_2 change	0.103 ± 0.001	0.089 ± 0.002	0.012 ± 0.001
Change in minimum sea ice extent (10^6 km^2)	Arctic (September)	0.98 ± 0.01	0.81 ± 0.02	1.66 ± 0.02
	Antarctic (March)	-0.13 ± 0.01	-0.16 ± 0.01	-0.07 ± 0.04
Precipitation changes (mm/day)	Global	-0.07 ± 0.01	-0.17 ± 0.03	-0.07 ± 0.01
	India (JJA months)	-0.50 ± 0.01	-0.23 ± 0.03	-0.68 ± 0.03
	Amazon (ASON months)	-0.02 ± 0.01	-0.45 ± 0.03	$+0.17 \pm 0.02$

Note. The error represents ± 1 standard error for each ensemble of results. All metrics are evaluated in the 2070–2089 period and compared with the 2010–2029 period when defined as change.
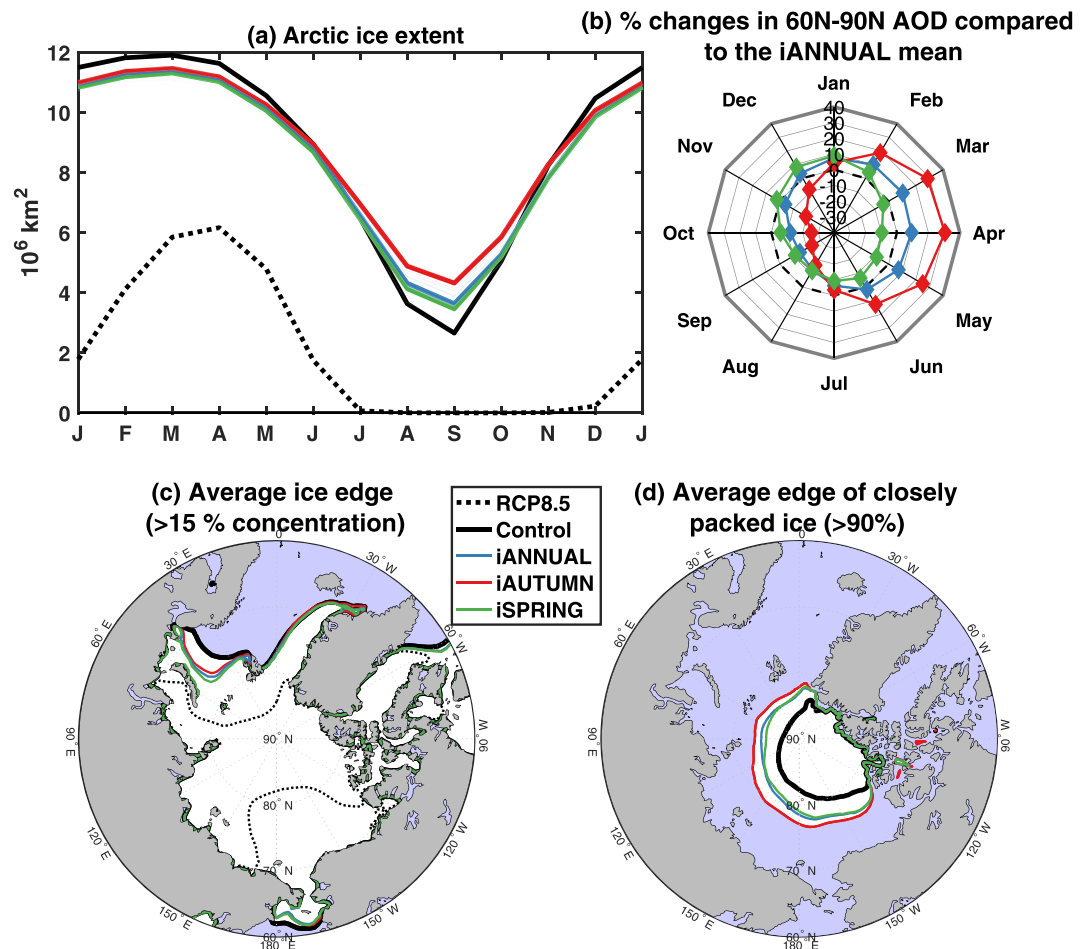

Figure 2. (a) Monthly sea ice extension for all periods in the Arctic (60°N–90°N) for the three injection strategies. Light lines represent single ensemble members, while thick lines represent the ensemble average. (b) Changes (in percent) in the monthly AOD (between 60°N–90°N) for the three cases, compared with the annual mean of the iANNUAL case. Bottom panels show the areas where, on average, sea ice coverage is present all year for the cases.
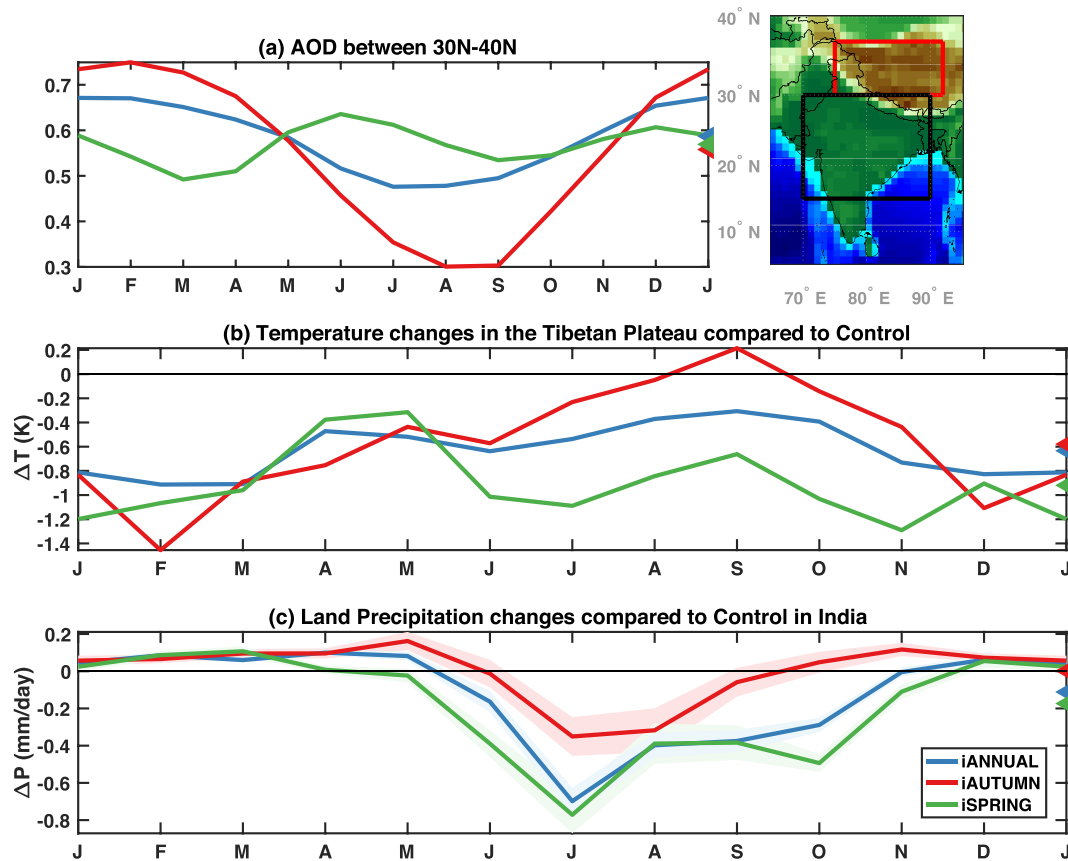
Figure 3. (a) Modeled seasonal AOD between 30°N and 40°N. (b) Changes in the surface temperature (K) in the Tibetan Plateau (average over the red box). (c) Modeled precipitation response (mm/day) over India (land average over the black box, shaded area represent ±1 standard error for each ensemble of results). Averages are always over the period 2070–2089 against the 2010–2029 control period and over all ensemble members. Colored triangles on the right-hand axis indicate the annual mean for the three cases.

et al. (2019). For Antarctic sea ice, no significant differences are present between the three scenarios, even though the resulting AOD is quite different (Figure S4).

Globally, the precipitation response appears to be similar between the three cases (Figure S5), including the shift in intertropical convergence zone and its seasonal extent. However, there are some regions where the precipitation response is significantly different. We show here two examples of regions where the injection strategies seem to have opposed effects. As a first example, we show the Indian region, where most precipitation occurs during the monsoon season, with agriculture strongly relying on it, and where under RCP8.5, an increase is expected in most CMIP5 simulations. In Simpson et al. (2019), a reduction in precipitation over June, July, and August (JJA) for the iANNUAL simulation was already observed. At least half of this change is shown to occur as a consequence of the stratospheric heating produced by the sulfate aerosols. When comparing the iANNUAL simulation with the two seasonal cases, however, we observe different results for them, with iAUTUMN showing almost no change over the region and iSPRING showing a further reduction.

Following previous analyses of the known drivers of precipitation over the Indian area (Rajagopalan & Molnar, 2013; Yanai & Wu, 2006), we show that the differences we find in the precipitation response to the different strategies can be partially explained by the changes in surface air temperature over the Tibetan Plateau (the sea surface temperature [SST] over the Indian Ocean is similar across the three simulations; it is the temperature difference that matters). We show in Figure 3 that the cause for the differences between the injection strategies is to be found in the different seasonality of the AOD between 10°N–30°N that, while resulting in very similar annual value, show a maximum in different months of the year. This produces strong differences in the seasonal temperatures over the Tibetan Plateau, especially during the monsoon season and in the months after; while all strategies overcool the area on an annual basis, iAUTUMN shows almost no overcooling over summer and autumn, thus leading to less changes in precipitation over the Indian region.
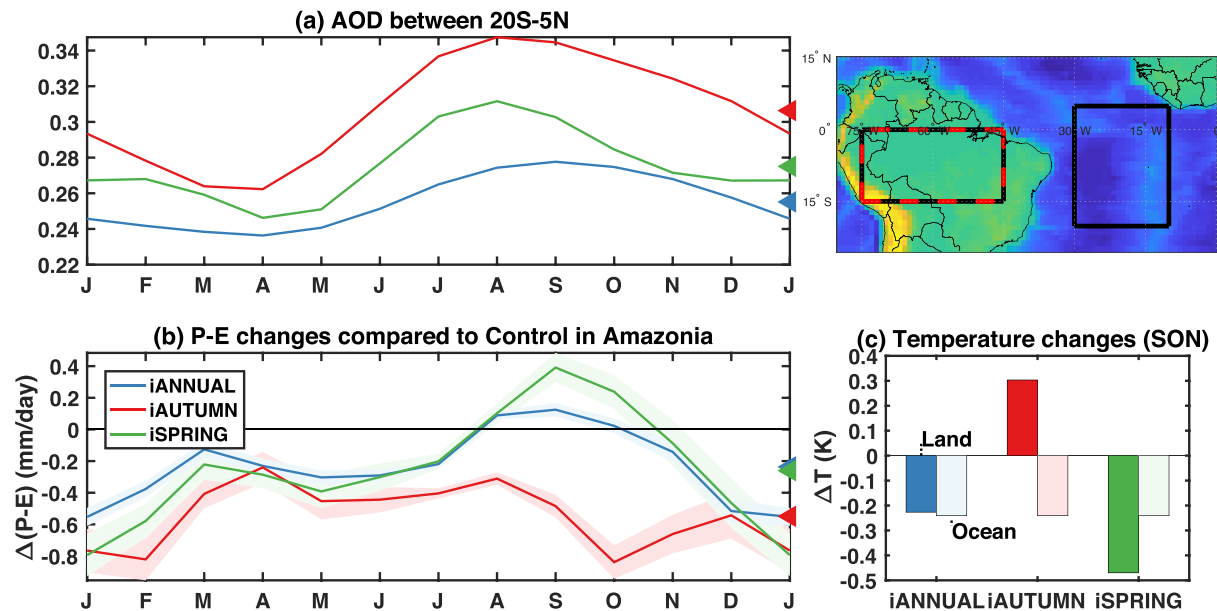
Figure 4. (a) Modeled seasonal AOD between 20°S and 5 N. (b) modeled P-E (precipitation minus evapotranspiration) response (mm/day) over the Amazon Basin (average over the red dashed box, shaded area represents ±1 standard error for each ensemble of results). (c) Changes in the surface temperature (K) over the Amazon Basin (average over the red dashed box) and over the Atlantic Ocean (average over the black box). Averages are always over the period 2070–2089 against the 2010–2029 control period and over all ensemble members. Colored triangles on the right-hand axis indicate the annual mean for the three cases.

As a second example, we show the precipitation changes over the Amazon Basin. Unlike India, a decline in precipitation is expected under RCP8.5, mostly due to the effect on plant physiology of the increased CO_2 levels (Langenbrunner et al., 2019). While the decrease in the wet period is already observed for the iANNUAL simulations (Simpson et al., 2019), it is also observed in the other two strategies and thus can be linked to changes produced by the stratosphere heating perturbations. Over the dry period, large differences are present between iSPRING and iAUTUMN, with the latter showing a large decrease in precipitation (Figure 4). The similarities in the SST response (driven by similar AOD values) rule out changes in the moisture advection from the Atlantic Basin (Jones et al., 2018), and in this case, the differences in land temperature appear to be the effect of moisture changes and not a cause. Unlike India, a direct causal link is harder to identify here, and the moisture changes seem to result from subtle changes in the modeled plant response, possibly due to a different ratio of diffuse to direct sunlight in some of the months.

As discussed in MacMartin et al. (2019), a larger ensemble size allows for a clearer identification of the forced response, and the three-member ensemble used here leads to higher standard errors compared with the 21-member GLENS ensemble (as shown in Table 2 and Figures 3 and 4). The key results shown here are computed as being statistically significant, when assuming that all 63 years (21 years each in three ensemble members) are statistically independent; they remain statistically significant even if only every fifth year of each 21-year period is considered. Multidecadal variability could nonetheless still play some role in the projected changes, and ultimate conclusions informing SAG policy will require larger ensembles and a wider range of explored strategies simulated in multiple climate models.

4. Conclusions

Discussing the possible impacts of a hypothetical future deployment of SAG introduces additional challenges compared with discussing the impacts of the increase in GHGs. First is because additional uncertainties are present when simulating SAG in climate models (Kravitz & MacMartin, 2020; MacMartin et al., 2015) compared with an increase in CO_2 in the atmosphere. Second is because unlike GHGs that quickly and efficiently mix in the atmosphere resulting in a more uniform forcing, the location(s) of the injection of SO_2 in the stratosphere results in important differences in the effects produced on the surface climate (Kravitz et al., 2019; MacMartin et al., 2017). It is therefore possible to devise injection strategies

depending on different climate goals (Tilmes, Richter, Kravitz, et al., 2018), trying to globally minimize the impacts that would inevitably happen due to the mismatch between the radiative forcing of CO_2 and that of the stratospheric sulfate (Govindasamy et al., 2000; Jiang et al., 2019).

We have shown here that by limiting injection to some portion of the year rather than all year long, it is possible to achieve similar global-scale climate objectives while at a more regional scale obtaining some significant differences in the surface climate response to the injections, in particular related to Arctic sea ice and precipitation. This further highlights the need to better understand the potential regional effects of SAG (Jones et al., 2018), but opens up the possibility of using this understanding to devise more complex strategies better capable of managing trade-offs and minimizing undesired impacts. To develop such strategies, there are three elements that need to be understood in depth: (i) how injection rates at different times and locations produce different spatiotemporal patterns of AOD (as in Visioni et al., 2019); (ii) how these patterns then affect the climate, both globally and regionally; and (iii) how confident we are in the outcomes obtained from a single model, compared with the eventual response of the climate. Especially for the last point, future volcanic eruptions and the discrepancies between the actual and modeled effects could improve our understanding of how and why their response might differ and how models can be improved to obtain more robust projections of eventual SAG deployments.

The actual AOD patterns do not quite match the patterns obtained by combining the results from single-point injections in Visioni et al. (2019) (see Figure S6), due to nonlinearities in both aerosol microphysics and stratospheric dynamics; however, over India and the Arctic, for example, the prediction is sufficient to correctly determine the seasonal variation of the overall AOD. If the mechanism that links the changes in the AOD pattern to some of the changes in surface climate can be understood (as is the case of Arctic sea ice, or changes to the Indian Monsoon), it may be possible to consider these changes as potential controllable outcomes of a SAG strategy, and not just as unavoidable "impacts."

Even keeping in mind the large uncertainties in the modeling of the aerosols and of their climate response (Kravitz & MacMartin, 2020) that might produce a different response in the real world compared with a climate simulation, this finding has strong implications for the potential governance of SAG. Envisioning an eventual governance for the deployment of SAG also means imagining a decision process related to the injection strategy: if multiple strategies can result (or are projected to result) in similar goals being achieved at a global scale, yet with different impacts in different regions, then various actors with particular interests might have divergent preferences over which strategy to use.

Conflict of Interest

The authors declare no conflict of interest.

Data Availability Statement

Simulation outputs used in this work are available for download here (http://www.cesm.ucar.edu/projects/community%2010projects/GLENS/) for the iANNUAL simulations and will be made available at https://ecommons.cornell.edu/ upon acceptance for all other simulations presented here.

References

Ban-Weiss, G. A., & Caldeira, K. (2010). Geoengineering as an optimization problem. *Environmental Research Letters*, *5*(3), 034009. https://doi.org/10.1088/1748-9326/5/3/034009

Cheng, W., MacMartin, D. G., Dagon, K., Kravitz, B., Tilmes, S., Richter, J. H., et al. (2019). Soil moisture and other hydrological changes in a stratospheric aerosol geoengineering large ensemble. *Journal of Geophysical Research: Atmospheres*, *124*, 12,773–12,793. https://doi.org/10.1029/2018JD030237

Crutzen, P. J. (2006). Albedo enhancement by stratospheric sulfur injections: A contribution to resolve a policy dilemma? *Climatic Change*, *77*(3–4), 211–220. https://doi.org/10.1007/s10584-006-9101-y

Fasullo, J. T., Simpson, I. R., Kravitz, B., Tilmes, S., Richter, J. H., MacMartin, D. G., & Mills, M. J. (2018). Persistent polar ocean warming in a strategically geoengineered climate. *Nature Geoscience*, *11*(12), 910–914. https://doi.org/10.1038/s41561-018-0249-7

Govindasamy, B., Caldeira, K., & Duffy, P. B. (2000). Geoengineering Earth's radiation balance to mitigate CO_2-induced climate change. *Geophysical Research Letters*, *27*(14), 2141–2144. https://doi.org/10.1029/1999GL006086

Jiang, J., Cao, L., MacMartin, D. G., Simpson, I. R., Kravitz, B., Cheng, W., et al. (2019). Stratospheric sulfate aerosol geoengineering could alter the high-latitude seasonal cycle. *Geophysical Research Letters*, *46*, 14,153–14,163. https://doi.org/10.1029/2019GL085758

Jones, A. C., Hawcroft, M. K., Haywood, J. M., Jones, A., Guo, X., & Moore, J. C. (2018). Regional climate impacts of stabilizing global warming at 1.5 K using solar geoengineering. *Earth's Future*, *6*, 230–251. https://doi.org/10.1002/2017EF000720

Kravitz, B., & MacMartin, D. G. (2020). Uncertainty and the basis for confidence in solar geoengineering research. *Nature Reviews Earth & Environment*, *1*(1), 64–75. https://doi.org/10.1038/s43017-019-0004-7

Kravitz, B., MacMartin, D. G., Wang, H., & Rasch, P. J. (2016). Geoengineering as a design problem. *Earth System Dynamics*, *7*(2), 469–497. https://doi.org/10.5194/esd-7-469-2016

Kravitz, B., MacMartin, D. G., Mills, M. J., Richter, J. H., Tilmes, S., Lamarque, J.- F., et al. (2017). First simulations of designing stratospheric sulfate aerosol geoengineering to meet multiple simultaneous climate objectives. *Journal of Geophysical Research: Atmospheres*, *122*, 12,616–12,634. https://doi.org/10.1002/2017JD026874

Kravitz, B., Macmartin, D. G., Tilmes, S., & Richter, J. H. (2019). Comparing surface and stratospheric impacts of geoengineering with different SO2 injection strategies. *Journal of Geophysical Research: Atmospheres*, *124*, 7900–7918. https://doi.org/10.1029/2019JD030329

Labitzke, K., & McCormick, M. P. (1992). Stratospheric temperature increases due to Pinatubo aerosols. *Geophysical Research Letters*, *19*(2), 207–210. https://doi.org/10.1029/91GL02940

Langenbrunner, B., Pritchard, M. S., Kooperman, G. J., & Randerson, J. T. (2019). Why does Amazon precipitation decrease when tropical forests respond to increasing CO_2? *Earth's Future*, *7*, 450–468. https://doi.org/10.1029/2018EF001026

Lawrence, M. G., Schäfer, S., Muri, H., Scott, V., Oschlies, A., Vaughan, N. E., et al. (2018). Evaluating climate geoengineering proposals in the context of the Paris Agreement temperature goals. *Nature Communications*, *9*(1), 3734. https://doi.org/10.1038/s41467-018-05938-3

Liu, X., Easter, R. C., Ghan, S. J., Zaveri, R., Rasch, P., Shi, X., et al. (2012). Toward a minimal representation of aerosols in climate models: Description and evaluation in the Community Atmosphere Model CAM5. *Geoscientific Model Development*, *5*(3), 709–739. https://doi.org/10.5194/gmd-5-709-2012

MacMartin, D. G., Keith, D. W., Kravitz, B., & Caldeira, K. (2013). Management of trade-offs in geoengineering through optimal choice of non-uniform radiative forcing. *Nature Climate Change*, *3*(4), 365–368. https://doi.org/10.1038/nclimate1722

MacMartin, D. G., Kravitz, B., & Rasch, P. J. (2015). On solar geoengineering and climate uncertainty. *Geophysical Research Letters*, *42*, 7156–7161. https://doi.org/10.1002/2015GL065391

MacMartin, D. G., Kravitz, B., Tilmes, S., Richter, J. H., Mills, M. J., Lamarque, J.- F., et al. (2017). The climate response to stratospheric aerosol geoengineering can be tailored using multiple injection locations. *Journal of Geophysical Research: Atmospheres*, *122*, 12,574–12,590. https://doi.org/10.1002/2017JD026868

MacMartin, D. G., Wang, W., Richter, J. H., Mills, M. J., Kravitz, B., & Tilmes, S. (2019). Timescale for detecting the climate response to stratospheric aerosol geoengineering. *Journal of Geophysical Research: Atmospheres*, *124*, 1233–1247. https://doi.org/10.1029/2018JD028906

Mills, M. J., Richter, J. H., Tilmes, S., Kravitz, B., MacMartin, D. G., Glanville, A. A., et al. (2017). Radiative and chemical response to interactive stratospheric sulfate aerosols in fully coupled CESM1 (WACCM). *Journal of Geophysical Research: Atmospheres*, *122*, 13,061–13,078. https://doi.org/10.1002/2017JD027006

Mills, M. J., Schmidt, A., Easter, R., Solomon, S., Kinnison, D. E., Ghan, S. J., et al. (2016). Global volcanic aerosol properties derived from emissions, 1990–2014, using CESM1 (WACCM). *Journal of Geophysical Research: Atmospheres*, *121*, 2332–2348. https://doi.org/10.1002/2015JD024290

National Research Council (2015). *Climate intervention: Reflecting sunlight to cool Earth*, (p. 234). Washington, DC: National Academies Press.

Niemeier, U., Schmidt, H., Alterskjaer, K., & Kristjánsson, J. E. (2013). Solar irradiance reduction via climate engineering: Impact of different techniques on the energy balance and the hydrological cycle. *Journal of Geophysical Research: Atmospheres*, *118*, 11,905–11,917. https://doi.org/10.1002/2013JD020445

Pitari, G., Aquila, V., Kravitz, B., Robock, A., Watanabe, S., Cionni, I., et al. (2014). Stratospheric ozone response to sulfate geoengineering: Results from the Geoengineering Model Intercomparison Project (GeoMIP). *Journal of Geophysical Research: Atmospheres*, *119*, 2629–2653. https://doi.org/10.1002/2013JD020566

Pitari, G., Di Genova, G., Mancini, E., Visioni, D., Gandolfi, I., & Cionni, I. (2016). Stratospheric aerosols from major volcanic eruptions: A composition-climate model study of the aerosol cloud dispersal and e-folding time. *Atmosphere*, *6*, 7. http://www, mdpi.com/2073-4433/7/6/75

Rajagopalan, B., & Molnar, P. (2013). Signatures of Tibetan Plateau heating on Indian summer monsoon rainfall variability. *Journal of Geophysical Research: Atmospheres*, *118*, 1170–1178. https://doi.org/10.1002/jgrd.50124

Richter, J. H., Tilmes, S., Mills, M. J., Tribbia, J. J., Kravitz, B., MacMartin, D. G., et al. (2017). Stratospheric dynamical response and ozone feedbacks in the presence of SO_2 injections. *Journal of Geophysical Research: Atmospheres*, *122*, 12,557–12,573. https://doi.org/10.1002/2017JD026912

Robock, A. (2000). Volcanic eruptions and climate. *Reviews of Geophysics*, *1998*, 191–219.

Simpson, I. R., Tilmes, S., Richter, J. H., Kravitz, B., MacMartin, D. G., Mills, M. J., et al. (2019). The regional hydroclimate response to stratospheric sulfate geoengineering and the role of stratospheric heating. *Journal of Geophysical Research: Atmospheres*, *124*, 12,587–12,616. https://doi.org/10.1029/2019JD031093

Tilmes, S., Fasullo, J., Lamarque, J.-F., Marsh, D. R., Mills, M., Alterskjaer, K., et al. (2013). The hydrological impact of geoengineering in the Geoengineering Model Intercomparison Project (GeoMIP). *Journal of Geophysical Research: Atmospheres*, *118*, 11,036–11,058. https://doi.org/10.1002/jgrd.50868

Tilmes, S., Richter, J. H., Kravitz, B., MacMartin, D. G., Mills, M. J., Simpson, I. R., et al. (2018). CESM1(WACCM) stratospheric aerosol geoengineering large ensemble (GLENS) project. *Bulletin of the American Meteorological Society*, *99*(11), 2361–2371. https://doi.org/10.1175/BAMS-D-17-0267.1

Tilmes, S., Richter, J. H., Mills, M. J., Kravitz, B., MacMartin, D. G., Garcia, R. R., et al. (2018). Effects of different stratospheric SO_2 injection altitudes on stratospheric chemistry and dynamics. *Journal of Geophysical Research: Atmospheres*, *123*, 4654–4673. https://doi.org/10.1002/2017JD028146

Visioni, D., MacMartin, D. G., Kravitz, B., Tilmes, S., Mills, M. J., Richter, J. H., & Boudreau, M. P. (2019). Seasonal injection strategies for stratospheric aerosol geoengineering. *Geophysical Research Letters*, *46*, 7790–7799. https://doi.org/10.1029/2019GL083680

Visioni, D., Pitari, G., & Aquila, V. (2017). Sulfate geoengineering: A review of the factors controlling the needed injection of sulfur dioxide. *Atmospheric Chemistry and Physics*, *17*(6), 3879–3889. https://doi.org/10.5194/acp-17-3879-2017

Visioni, D., Pitari, G., Aquila, V., Tilmes, S., Cionni, I., De Genova, G., & Mancini, E. (2017). Sulfate geoengineering impact on methane transport and lifetime: Results from the Geoengineering Model Intercomparison Project (GeoMIP). *Atmospheric Chemistry and Physics*, *17*(18), 11,209–11,226. https://doi.org/10.5194/acp-17-11209-2017

Visioni, D., Pitari, G., Tuccella, P., & Curci, G. (2018). Sulfur deposition changes under sulfate geoengineering conditions: Quasi-biennial oscillation effects on the transport and lifetime of stratospheric aerosols. *Atmospheric Chemistry and Physics*, *18*(4), 2787–2808. https://doi.org/10.5194/acp-18-2787-2018

Yanai, M., & Wu, G.-X. (2006). Effects of the Tibetan Plateau. In B. Wang (Ed.), *The Asian monsoon*, (pp. 513–549). Berlin, Heidelberg: Springer.

Zambri, B., & Robock, A. (2016). Winter warming and summer monsoon reduction after volcanic eruptions in Coupled Model Intercomparison Project 5 (CMIP5) simulations. *Geophysical Research Letters*, *43*, 10,920–10,928. https://doi.org/10.1002/2016GL070460